

# *IET Renewable Power Generation*

## **Special Issue Call for Papers**

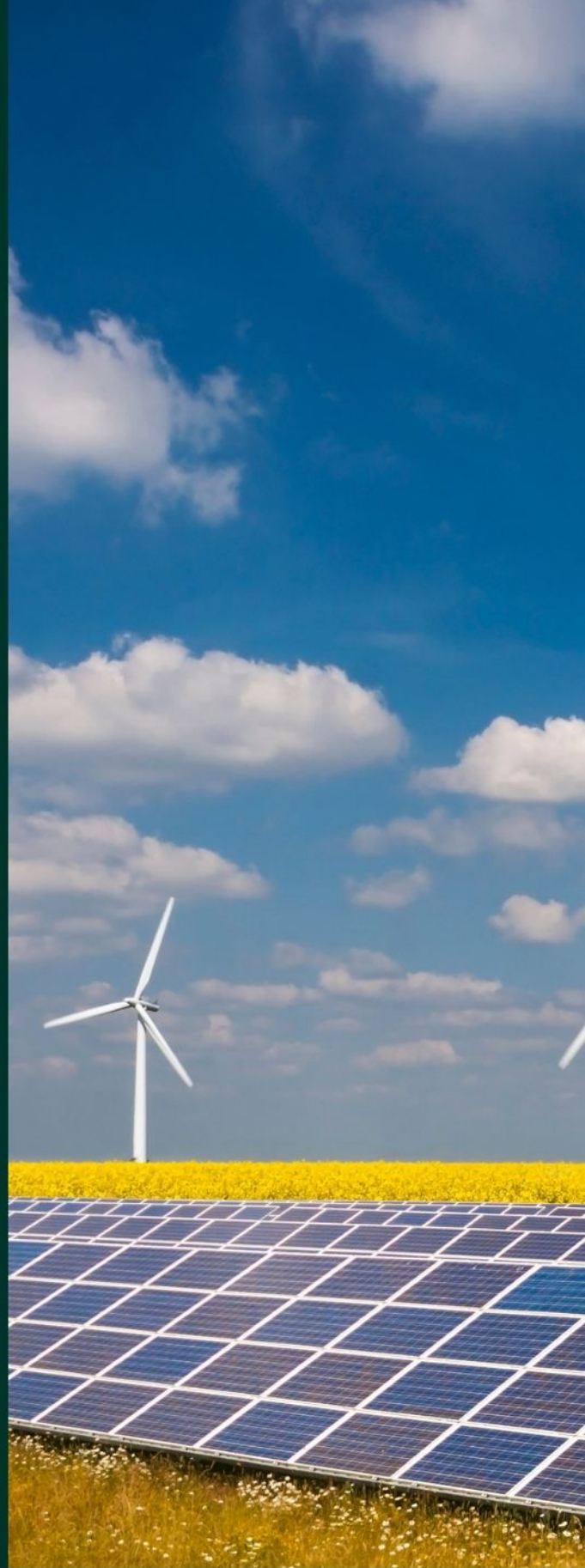
---

**Be Seen. Be Cited.  
Submit your work to a new  
IET special issue**

Connect with researchers and  
experts in your field and  
share knowledge.

Be part of the latest research  
trends, faster.


[Read more](#)



The Institution of  
Engineering and Technology

## ORIGINAL RESEARCH

# Effective demand response and GANs for optimal constraint unit commitment in solar-tidal based microgrids

Mohammadamin Mobtahej<sup>1</sup>  | Khodakhast Esapour<sup>2</sup> | Seyede Zahra Tajalli<sup>2</sup> |  
Mojtaba Mohammadi<sup>2</sup>

<sup>1</sup> School of Electrical Engineering, Kazeroon Islamic Azad University, Fars, Iran

<sup>2</sup> Department of Electrical Engineering, Isfahan (Khorasgan) Branch, Islamic Azad University, Isfahan, Iran

## Correspondence

Mohammadamin Mobtahej, School of Electrical Engineering, Kazeroon Islamic Azad University, Fars, Iran.  
Email: Aminmobtahej@gmail.com

## Abstract

A new approach for optimal demand response program (DRP) in the microgrid considering the high penetration of the solar energy and tidal units as significant and popular renewable sources in the system is proposed here. The proposed method makes use of a multi-objective problem (MOP) to not only minimize the total operation cost of the scheduling problem but also mitigate the high risk of the interruption in power delivery due to the components failure rate and long repairing rates. Considering the high complexity and nonlinearity of the formulation, a novel heuristic method based on the firefly algorithm is introduced to solve the problem without any assumption or killing the accuracy. In addition, a dynamic three-phase correction (DPC) formulation is proposed which can help to increase the global search characteristics of the method when boosting the convergence capability of the model. Due to the hard predictability nature of the solar irradiance, a deep learning model based on generative adversarial networks (GAN) is presented to predict the output power of the solar and tidal units properly. The high performance and feasibility of the proposed multi-layer problem are assessed on an IEEE test system.

## 1 | INTRODUCTION

Civilization and modernization have increased the number and population of cities in the new century. It is estimated that over 50% of the world population would live in the cities by 2050. This would increase the demand in all aspects including the electrical and thermal loads severely. In this situation, the power system as a big legacy system would survive in its current form due to the necessity of continuous power delivery and high capital cost for the renewal [1–3]. This situation shows that all parts of the power system including the smart grids, microgrids, distribution systems, transmission systems, and generations would experience load growth at a rapid rate [4]. In this situation, optimal scheduling and unit commitment of the grid is a critical task that must be taken into consideration. Many researchers have focused on this topic recently. In [1] a secured optimal scheduling framework for optimal operation of hybrid microgrids in both islanded and grid-connected modes is proposed. In [4], the operation of the microgrid is formulated as a single objec-

tive problem that is solved using heuristic optimization algorithms. Another issue regarding the operation of microgrids is heavy peak loads. In order to overcome the severe peak loads safely and without load shedding, the demand response program (DRP) will play a critical and vital role [5, 6]. By definition, DRP is the mitigation in the electrical load demand for reducing the peak demand or avoiding the system to enter the emergency status from the normal status [7]. Therefore, it might be assumed as a technical and economic tool for reducing the power losses and costs and avoiding the investment costs in the long term. Such a cost-effective tool adds to the generation capacity and can handle the demand spikes [8].

In recent years, many pieces of research have been implemented to check different aspects of the DRP. In [9], DRP is used in a probabilistic fuzzy method for benefiting both the electrical customers and the main grid. The model performance is demonstrated on a remotely islanded solar-diesel-battery grid. In [10], DRP is joint with battery storage in a combined heat and power system which could mitigate the operation cost by 6.5%

This is an open access article under the terms of the [Creative Commons Attribution-NonCommercial-NoDerivs](https://creativecommons.org/licenses/by-nc-nd/4.0/) License, which permits use and distribution in any medium, provided the original work is properly cited, the use is non-commercial and no modifications or adaptations are made.

© 2021 The Authors. *IET Renewable Power Generation* published by John Wiley & Sons Ltd on behalf of The Institution of Engineering and Technology.

and 11.7%, respectively. Moreover, it is shown that the combined model could minimize the energy losses and costs, simultaneously. In contrast to the conventional DRP which makes a load reduction, it is shown in [11] that an effective DRP should also play a boosting role by adding the load demand at off-peak load hours. In fact, positive demand response can reduce the generator ramping needs and thus mitigate the overall prices during peak hours. A new two-layer problem formulation is devised in [12] which assesses the effect of the incentive tools in the DRP on the operating costs. The simulation results on the IEEE 33-bus system reveals about a 19% reduction in the cost and a 45% reduction in the total emission. In [13], the effect of DRP is investigated in two forms of shiftable loads and curtailable loads in the microgrids. It is shown that DRP can make a positive effect on the bus voltage profile as an indirect effect and thus reduce the power losses and costs. It is seen that DRP can be a big asset to electric vehicles by releasing the occupied capacity of the feeders in the microgrid. These researches advocate the positive role of the DRP in the power system, ranging from the low voltage of distribution grids to the high voltage of the transmission systems.

The recent progress in renewable energy resources could facilitate the way for the high penetration of renewable energy sources as a flexibility tool to the power grids. With a sharp focus on the high polluting fossil fuel-based units, the renewable energy concept has attained attractive progress in reducing the losses, mitigating the costs, enhancing the reliability and power quality, decreasing air pollutions, and improving the voltage profile [14–17]. Unfortunately, the high amount of uncertainty injected by the renewable energy sources affects not only the DRP but also the operation and management policies in the power system. Therefore, this paper investigates the optimal DRP in the optimal scheduling of the units in the presence of high penetration of solar units and tidal turbines in a microgrid. In this regard, a multi-objective problem (MOP) is designed wherein the first layer is in charge of optimizing the operation costs. In the other layers, the length and frequency of interruptions are estimated in the worst case and it is tried to enhance this worst-case scenario using the optimal scheduling and DRP. Since heuristic algorithms are currently among the best solutions for non-linear optimization problems [15], in this paper a novel approach is proposed to solve the MOP in this work. Owing to the model complexity, a new corrected firefly algorithm [18] (CFA) is introduced to search for the optimal global solution in the constrained and feasible space of the problem. A novel dynamic three-phase correction (DPC) model is suggested for adding to the fireflies diversity in the population and increasing the searchability and convergence rate. In order to reduce the uncertainty effects, a deep learning model using the generative adversarial network (GAN) [19] is proposed to predict tidal and solar power accurately. Generally, in comparison to existing works, this work proposes several novel methods for microgrid operation. In this work, a deep learning-based framework for unit commitment and optimal scheduling of microgrids in presence of demand response technology and renewable sources (i.e. photovoltaic (PV) and tidal units) is proposed. Also, a novel optimization technique based on the Firefly algo-

rithm is developed to solve the operation problem of the system and minimize the system's cost objective function. Additionally, in this work the powerful deep learning model GAN is utilized for PV and tidal forecasting. Therefore, the key contributions of the work are as follows:

- Introducing a new MOP model for the DRP and optimal scheduling of the microgrids in the presence of solar and tidal units.
- Proposing an effective CFA for the optimal solving of the problem without any assumption or simplification.
- Developing a deep GAN-based approach for predicting the output power of solar and tidal units, precisely.

The performance and quality of the proposed MOP model are assessed on an IEEE standard case study.

The rest of this paper is organized as: Section 2 explains the proposed MOP including the objectives and constraints. Section 3 describes the managing framework based on CFA and GAN. The results and discussions are provided in Section 4. Finally, Section 5 shows the conclusions and outcomes of the research.

## 2 | PROBLEM FORMULATION

In this part, the proposed MOP is described according to the objective function and constraints. In the proposed model, the initial layer optimizes the cost of the optimal scheduling neglecting the component failure effects. In the second layer, the reliability indices of (AENS) and system average interruption duration index (SAIDI) are mitigated according to the uncertainty of failure rate and repair rate time.

### 2.1 | Objective functions

The total operation cost consists of the cost of power produced by the units to support the microgrid load demand, cost of power losses, and cost of switching as follows:

$$Cost = \sum_t \sum_i F_i(P_{it}) + \sum_t \Phi_t^M P_t^M + \sum_t \sum_{m \in L} (\chi_{mt}^1 + \chi_{mt}^2) \lambda^{RCS} \quad (1)$$

In (1), the first term refers to the cost of DGs, start-up and shut-down cost; the second term refers to the cost of power purchasing from the utility (when the microgrid is in connected mode) and the last term refers to the cost of switching. Switching is a useful and strategic tool for the operator to change the microgrid topology and power flow in accordance with the objective function and preferences. Such a strategy can reduce the losses, enhance the reliability indices and mitigate the cost and capital costs.

The second objective function is the AENS which calculates the average energy which is estimated to not be supplied by the microgrid and can affect the reliability of the system and the sustainability of the electrical power supply.

$$AENS = \frac{\sum_{n \in B} Lc_n \Gamma_n}{\sum_{n \in B} N_n^C} \quad (2)$$

The third objective function is SAIDI which estimates the average time which the system may experience after a fault occurs in the system. This is a popular index for showing the electrical services to the customers and is calculated yearly.

$$SAIDI = \frac{\sum_{n \in B} \Gamma_n N_n^C}{\sum_{n \in B} N_n^C} \quad (3)$$

## 2.2 | Limitation and constraints

The above objectives would be optimized when meeting the equality and inequality constraints:

### • Power unit limits

In (4), the dispatchable units are restricted to produce in their capacity range. The minimum up and down rate for power generation increase or decrease is shown in (5) and (6). The minimum up and downtime are shown in (7) and (8).

$$P_i^{\min} v_{it} \leq P_{it} \leq P_i^{\max} v_{it} \quad \forall i \in G, \forall t \quad (4)$$

$$P_{it} - P_{i(t-1)} \leq \mathfrak{R}^u_i \quad \forall i \in G, \forall t \quad (5)$$

$$P_{i(t-1)} - P_{it} \leq \mathfrak{R}^D_i \quad \forall i \in G, \forall t \quad (6)$$

$$T_{it}^{on} \geq UT_i(v_{it} - v_{i(t-1)}) \quad \forall i \in G, \forall t \quad (7)$$

$$T_{it}^{off} \geq DT_i(v_{i(t-1)} - v_{it}) \quad \forall i \in G, \forall t \quad (8)$$

### • Battery storage unit

The maximum charging/discharging rate of the units is presented in (9) and (10). The binary variables  $u$  and  $v$  show the charging/discharging status of the battery. The amount of energy stored in the battery is calculated according to the efficiency (12). It is clear that a battery has a limited capacity for energy storage (13). In order to avoid fast aging of the battery, a minimum charging/discharging time is considered for the battery (14) and (15).

$$P_{st} \leq P_{st}^{dcb, \max} v_{st} - P_{st}^{dcb, \min} u_{st} \quad \forall s \in S, \forall t \quad (9)$$

$$P_{st} \geq P_{st}^{dcb, \min} v_{st} - P_{st}^{dcb, \max} u_{st} \quad \forall s \in S, \forall t \quad (10)$$

$$u_{st} + v_{st} \leq 1 \quad \forall s \in S, \forall t \quad (11)$$

$$B_{st} = B_{s(t-1)} - \frac{P_{st} u_{st} \tau}{\eta_s} - P_{st} v_{st} \tau \quad \forall s \in S, \forall t \quad (12)$$

$$B_s^{\min} \leq B_{st} \leq B_s^{\max} \quad \forall s \in S, \forall t \quad (13)$$

$$T_{st}^{ch} \geq MC_s(u_{st} - u_{s(t-1)}) \quad \forall s \in S, \forall t \quad (14)$$

$$T_{st}^{dch} \geq MD_s(v_{st} - v_{s(t-1)}) \quad \forall s \in S, \forall t \quad (15)$$

### • DRP limits

In order to attend the DRP, Equations (16) to (18) are deployed to show the limited power demand of the load (16), the total energy required in a specific time range (17), and the minimum up time for the dispatchable loads (18).

$$PD_{dt}^{\min} \zeta_{dt} \leq PD_{dt} \leq PD_{dt}^{\max} \zeta_{dt} \quad \forall d \in D, \forall t \quad (16)$$

$$\sum_{t \in [\epsilon, \nu]} PD_{dt} = E_d \quad \forall d \in D \quad (17)$$

$$T_{dt}^{on} \geq MU_d(\zeta_{dt} - \zeta_{d(t-1)}) \quad \forall d \in D, \forall t \quad (18)$$

### • Microgrid structure modelling

In order to meet the generation and consumption balance, (19) and (20) are used in this paper. It is clear that the normal active and reactive power flow equations are considered in this part. The microgrid is technically able to exchange a limited amount of power with the utility (21). In order to show the switching process, an auxiliary variable  $\beta_{mnt}$  is used to show the On or Off status of the line. Therefore, the maximum and minimum power flow rate in a feeder is restricted by (22) to (25). In (26), the maximum voltage deviation from the rate value is restricted.

$$\sum_{i \in B_m} P_{it} + \sum_n PL_{mnt} + P_t^M = \sum_d PD_{dt} \quad \forall t, \forall m \quad (19)$$

$$\sum_{i \in B_m} Q_{it} + \sum_n QL_{mnt} + Q_t^M = \sum_d QD_{dt} \quad \forall t, \forall m \quad (20)$$

$$-u^M P^{M,\min} \leq P_t^M \leq u^M P^{M,\min} \quad \forall t \quad (21)$$

$$\begin{aligned} -M(1 - \beta_{mnt}) &\leq PL_{mnt} - V_{mt} V_{nt} Y_{mn} \cos(\theta_{mn} + \delta_{mt} - \delta_{nt}) \\ &\leq M(1 - \beta_{mnt}) \quad \forall mn \in L, \forall t \end{aligned} \quad (22)$$

$$-PL_{mn}^{\max} \beta_{mnt} \leq PL_{mnt} \leq PL_{mn}^{\max} \beta_{mnt} \quad \forall mn \in L, \forall t \quad (23)$$

$$\begin{aligned} -M(1 - \beta_{mnt}) &\leq QL_{mnt} - V_{mt} V_{nt} Y_{mn} \sin(\theta_{mn} + \delta_{mt} - \delta_{nt}) \\ &\leq M(1 - \beta_{mnt}) \quad \forall mn \in L, \forall t \end{aligned} \quad (24)$$

$$-QL_{mn}^{\max} \beta_{mnt} \leq QL_{mnt} \leq QL_{mn}^{\max} \beta_{mnt} \quad \forall mn \in L, \forall t \quad (25)$$

$$V_m^{\min} \leq V_{mt} \leq V_m^{\max} \quad \forall m \in B \quad (26)$$

- Switching constraints

In order to avoid fast degradation of the switches, we need to avoid a high number of operations in the microgrid. Therefore, (27) to (29) would limit the maximum number of switching in the microgrid. Moreover, the microgrid structure and its radiality should be preserved after each switching as in (30).

$$\chi_{mnt}^1 \geq \beta_{mnt} - \beta_{mn(t-1)} \quad \forall mn \in L, \forall t \quad (27)$$

$$\chi_{mnt}^2 \geq \beta_{mn(t-1)} - \beta_{mnt} \quad \forall mn \in L, \forall t \quad (28)$$

$$\sum_t (\chi_{mnt}^1 + \chi_{mnt}^2) \leq N_{switching}^{\max} \quad \forall mn \in L \quad (29)$$

$$\sum_{mn \in Q} \beta_{mnt} \leq \omega_L - 1 \quad \forall q, \forall t \quad (30)$$

### 3 | PROPOSED INTELLIGENT MODEL

In this section, the proposed deep learning-based framework using GAN and CFA is explained. In the first part, CFA is described as the optimizer along with a dynamic three-phase correction (DPC) method. In the next part, the GAN model is described as the prediction solution for the solar and tidal units.

#### 3.1 | Corrected firefly algorithm

The firefly algorithm is a heuristic method that uses the living habits of fireflies in tropical countries to attract neighbouring insects. This algorithm can solve nonlinear and non-convex constrained optimization methods without any simplification or assumption in the problem formulation. A firefly in this algorithm represents a promising solution in the feasible problem space which can be either an optimal or non-optimal solution. The improvisation stage in the firefly algorithm is in charge of growing the population to a level that all solutions are near the optimal solution. Fundamentally, this algorithm works based on the firefly brightness as a representative of its attractiveness. In the beginning, a set of fireflies (solutions) are generated in the problem space. After calculating the objective function value for the fireflies  $X_j$  and sorting them, the best solution  $X_g$  is stored. It is now the time to enhance the firefly population based on their brightness. Therefore, the first stage is to compute the brightness of a firefly as below:

$$I(r) = \frac{I_s}{r^2} \quad (31)$$

As it can be seen from (31), the brightness of a firefly is reduced as the distance  $r$  increases. Considering the absorption coefficient for the light, the light value can be measured as below:

$$I = I_0 e^{-\gamma r} \quad (32)$$

One might reformulate the light value of a firefly using the Gaussian concept:

$$I(r) = \frac{I_0}{1 + \gamma r^2} \quad (33)$$

Therefore, we will show the firefly brightness according to the light value as below:

$$\Delta(r) = \Delta_0 \times e^{-\gamma r^2} \quad (34)$$

The first question is to compute the distance between any two fireflies in the Cartesian frame as below:

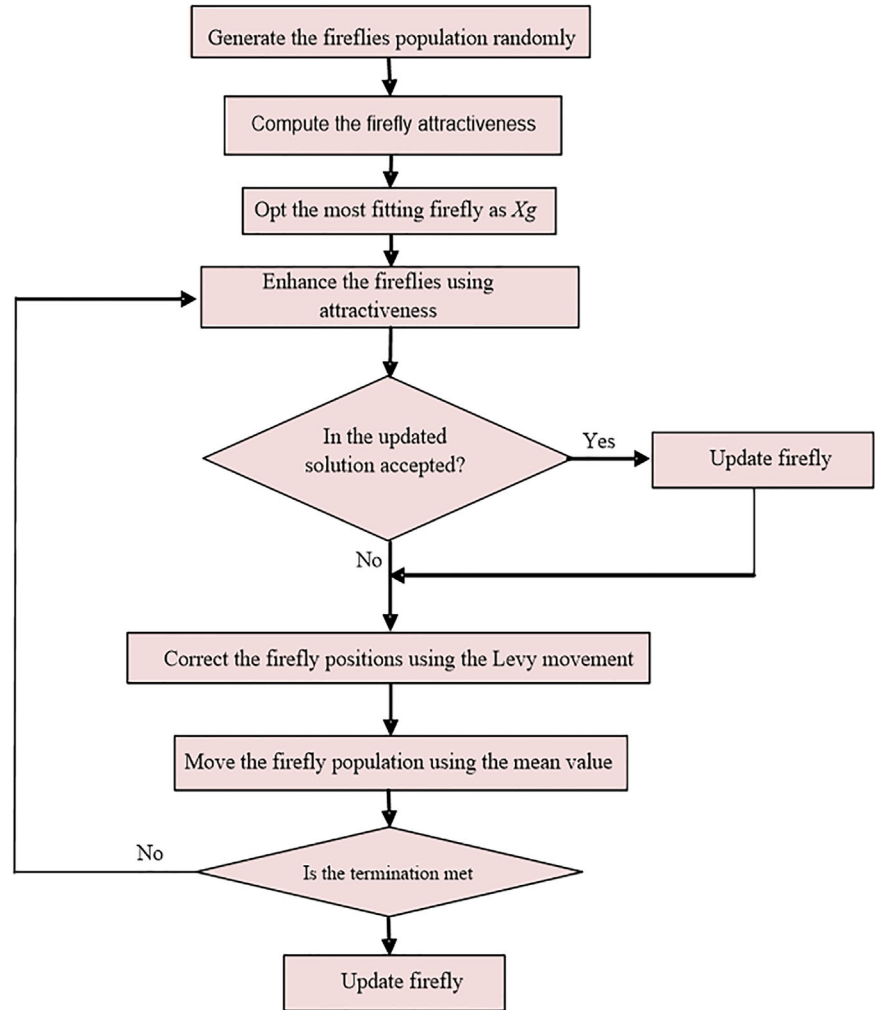
$$r_{ij} = |X_i - X_j| = \sqrt{(x_{i,1} - x_{j,1})^2 + (x_{i,2} - x_{j,2})^2} \quad (35)$$

It is time to update the position of all fireflies using the above brightness. Therefore, a firefly with high attractiveness would attract the other firefly with less attractiveness as below:

$$X_i = X_i + \Delta_0 \times e^{-\gamma r^2} (X_j - X_i) + \alpha(rand - 0.5) \quad (36)$$

This article suggests a correction method for the firefly algorithm to amend the improvisation stage using the local search mechanisms. To this end, a new method using the Levy action

FIGURE 1 The proposed CFA flowchart



is deployed to reinforce the slow movements around the optimal solution as below:

$$L^l \text{vy}(\rho) \sim \tau = l^{-\rho}; \quad (1 < \rho \leq 3) \quad (37)$$

where  $\rho$  is a random constant. By the above equation, a new promising optimal solution is generated as follows:

$$X_i^l = X_i^{l-1} + \varphi_1 \oplus L^l \text{vy}(\rho) \quad (38)$$

As it can be seen from (38), a local searching is implemented in the near neighbouring of each firefly to upgrade its position. This is so important since the original firefly algorithm does not have any local search tool.

In a second try, we enhance the convergence rate of the algorithm by shifting the mean of the fireflies' positions toward the best fitting solution  $X_g$  as below:

$$X_i^l = X_i^{l-1} \times l^{-0.01l} \times (X_g - M_D) \quad (39)$$

Figure 1 shows the flowchart of the proposed CFA.

### 3.2 | Deep generative adversarial network

In order to predict the output power of the solar panel and tidal units, there is an urgent need for a precise and accurate method. We propose the GAN model due to the competing networks which it uses in the game to produce the most fitting values for the parameters. A GAN model belongs to the class of machine learning methods which includes a generative model (GM) and a discriminative model (DM) to learn new data with varied statistical features. This is called zero-sum gaming with the GM trying to fool the DM through some fake data based on the Gaussian noise signal. Therefore, one can see that each player tries to amend its behaviour (which is the network's parameters values) intelligently based on the reaction of the other player. Figure 2 shows the structure of a GAN model.

The DM would compare the generated data with the real data and returns a probability between 0 and 1 to show the fake level of the data. Such a bidirectional interaction would continue until the returning probability becomes zero. In order to formulate the GAN, initially, a random signal  $G(N)$  is generated with the probability  $P_G(N)$ . After signal generation, the DM receives two inputs  $P_G(N)$  and  $P_R(x)$ , and tries to match  $P_G(N)$  on each

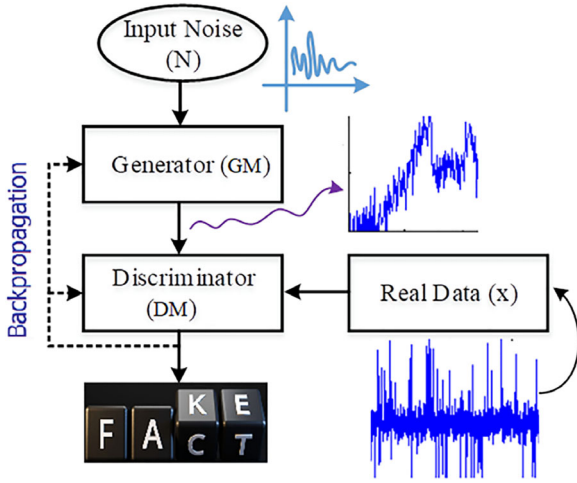


FIGURE 2 GAN model concept and structure

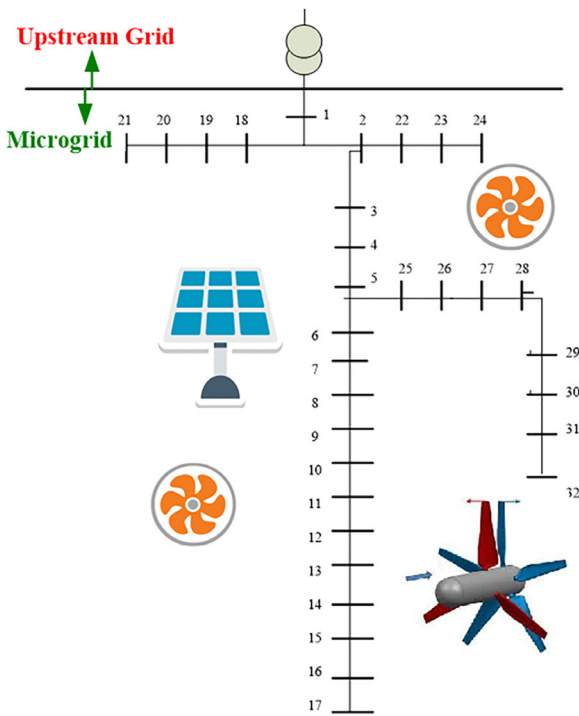


FIGURE 3 Single-line diagram of the test microgrid

TABLE 1 Microgrid structure including the generators, loads, and storages

Unit	Cost coefficient (\$/kWh)	Capacity limits (kW)	Least up/down hours (h)	Ramp up/down rate (kW/h)
DG1	0.153	1000–3000	2	1400
DG2	0.143	1000–2000	2	1400
DG3	0.204	700–2500	3	1200
DG4	0.191	700–2500	2	1000
WT	–	0–1700	–	–
PV	–	0–2200	–	–

TABLE 2 Battery storage system data

Storage	Capacity (kWh)	Min-max charging/ discharging power (kW)	Min charging/ discharging time (h)
ESS	1500	40–200	3

the real data. The DM would determine whether the signal is real or fake and this decision would affect both networks training. The difference between the  $P_R(x)$  and  $P_G(N)$  is considered as the error signal. Through a recursive process, and in each iteration, the error signal of the DM is returned to the GM. When the GM receives the error signal, it would attempt to produce data with as much similar distribution as to the real data. On the other hand, the DM adds up to its sensitivity and peruses ways to check and recognize fake data more accurately. This would result in a min-max equation wherein the feeding signal  $x$  and the DM parameters  $\theta^{(D)}$  are trained as below:

$$V(D, \theta^{(D)}) = -E_{x \sim P_R(x)} [\log D(x)] - E_{N \sim P_G(N)} [\log (1 - D(G(N)))] \quad (40)$$

In a similar interpretation, the GM with the parameter set  $\theta^{(G)}$  would be trained as below:

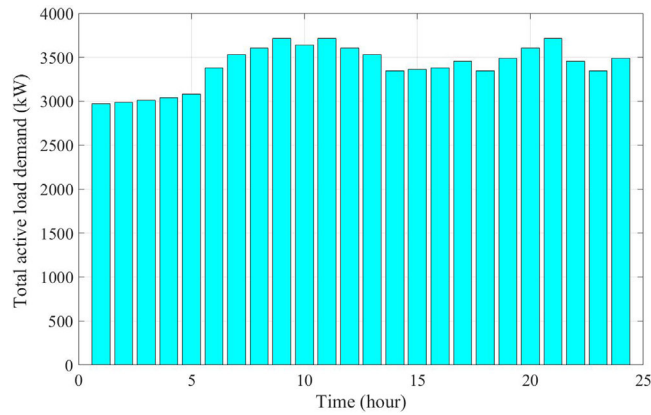
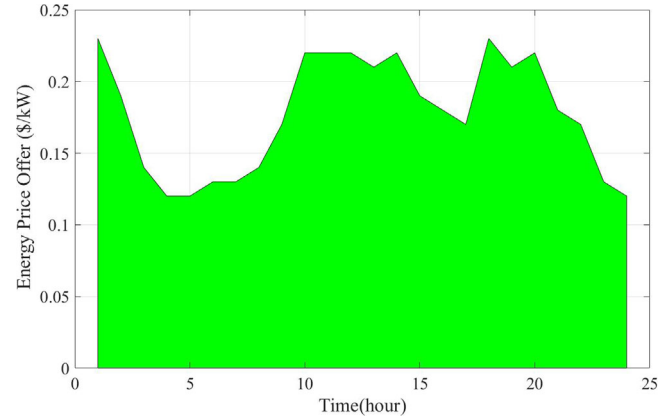
$$V(G, \theta^{(G)}) = E_{N \sim P_G(N)} [\log (1 - D(G(N)))] \quad (41)$$

Therefore, both GM and DM try to train with respect to the reaction of the competitor. It means that the GM tries to optimize the  $V^{(G)}(\theta^{(G)}, \theta^{(D)})$  by adjusting the values in  $\theta^{(G)}$  and assuming constant values in  $\theta^{(D)}$ . The same story exists for the DM  $V^{(D)}(D^{(G)}, \theta^{(D)})$  which tries to adjust the  $\theta^{(D)}$  for constant  $\theta^{(G)}$ . The final formulation is a combinatorial equation as below:

$$\min_G \max_D V(D, G) = E_{x \sim P_R(x)} [\log D(x)] + E_{N \sim P_G(N)} [\log (1 - D(G(N)))] \quad (42)$$

**TABLE 3** Loads attending the DRP in microgrid

Bus	Capacity limits (kW)	Total obligatory energy (kWh)	Available times (h)	Least uptime (h)
3	0–90	360	10–13	1
13	0–80	320	16–20	1
18	20–80	240	12–15	1
24	10–50	300	1–24	24
31	20–60	300	13–24	12

**FIGURE 4** Total Load Demand of the microgrid**FIGURE 5** Hourly forecast energy price

## 4 | EXPERIMENTAL RESULTS

In this section, the proposed model is applied and analysed on the IEEE 33-bus test system [19, 20]. In the test microgrid, there is 1 solar panel, 1 tidal turbine, 1 battery, and 4 dispatchable units. For the DRP, there are five buses with adjustable loads suitable for DRP and 27 buses with static loads. The microgrid is connected to the main grid through a circuit breaker and thus it is able to move into the islanding mode when there is no need to power exchange or in emergency cases. Figure 3 shows the one-diagram shape of the system. Tables 1 to 3 show the system characteristics for power units, generators, and loads [21].

In order to attend the DRP, there are five bus candidates which attend the demand response for peak load shaving and reducing the microgrid costs. Table 3 shows the location, capacity, and energy specifications of these loads. Moreover, Figures 4 and 5 show the forecast values of the load demand and the market bidding price over 24 h.

In the first phase, we need to predict the output power of the tidal unit and the solar panel using the GAN model. To this end, the historical data of the two solar and tidal sites are used over 1 year and the target history is the next 24 h. In order to check the model accuracy and performance quality, some indices are used in this paper as follows:

- Relative percentage error:

$$\sigma_k\% = \frac{|\bar{Y}_k - Y_k|}{Y_k} \times 100, k = 1, 2, \dots, N_{ts} \quad (43)$$

- Mean absolute percentage error (MAPE):

$$MAPE\% = \frac{1}{N_{ts}} \sum_{k=1}^{N_{ts}} \sigma_k \quad (44)$$

- Root mean square error (RMSE):

$$RMSE = \sqrt{\frac{1}{N_{ts}} \sum_{k=1}^{N_{ts}} \sigma_k^2} \quad (45)$$

- Maximum absolute relative percentage error (MARPE):

$$MARPE = \max \left( \left| 100 \times \frac{\bar{Y}_k - Y_k}{Y_k} \right| \right), i = 1, 2, \dots, N_{ts} \quad (46)$$

Tables 4 and 5 provide the prediction results for the photovoltaic unit and the tidal unit over 24 h using the GAN model, respectively. For a better comparison, the results are compared to the autoregressive (AR), artificial neural network (ANN),



**TABLE 4** Photovoltaic system output power prediction using GAN for 24 h

Method	MAPE (%)	MARPE	RMSE
AR	2.1673	4.9568	2.7331
ANN	1.8223	4.0386	2.2850
SVR	1.3308	3.1173	2.1673
Proposed method	0.5167	0.7337	0.6272

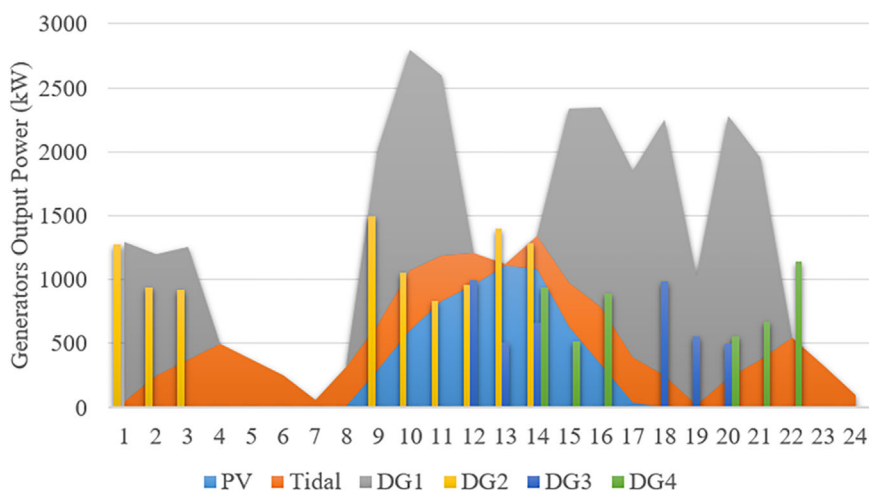
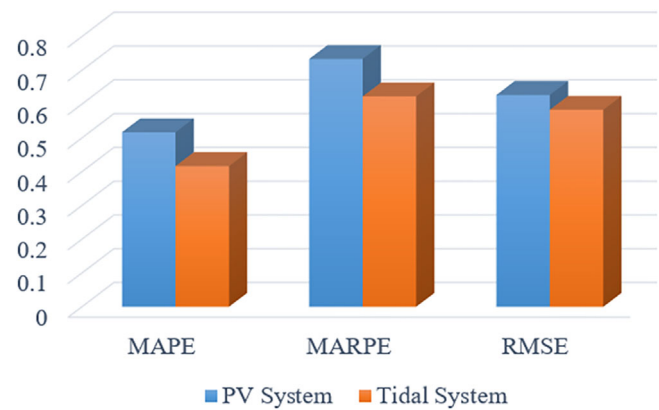
**TABLE 5** Tidal system output power prediction using GAN for 24 h

Method	MAPE (%)	MARPE	RMSE
AR	1.9360	3.3963	2.6835
ANN	1.6204	3.1647	2.4270
SVR	1.2361	2.0633	2.2887
Proposed method	0.4165	0.6227	0.5831

and support vector regression (SVR). As it can be seen from the results, the GAN model shows superior results and higher accuracy over the AR, ANN, and SVR methods. In addition, it is seen that the RMSE is low enough in both cases which shows the high robustness of the prediction method. By comparing Tables 4 and 5, one can conclude that the tidal unit output power is easier to predict rather than the photovoltaic output power.

Figure 6 is used to compare the MAPE, MARPE and RMSE results for the prediction of the PV and tidal system using the proposed method. According to these results, the prediction results for tidal unit are better than the PV unit which shows the higher complexity of PV dataset for the prediction. Overall, the proposed prediction model shows appropriate performance for all cases.

So far, the GAN model accuracy is validated. In order to check the microgrid power scheduling model, Figure 7 shows the optimal output power of the unit in the grid-connected mode. As it can be seen in the figure, the photovoltaic unit and the tidal are shown as filled curves. The dispatchable units with

**FIGURE 7** Power dispatch of units over 24 h in the grid-connected mode**FIGURE 6** The comparison of the prediction results by the proposed method for PV and tidal systems

lower prices are producing power at a higher amount rather than the non-dispatchable units. This is due to the nature of renewable sources which are not allowed to produce higher than a percentage due to the unstable and random characteristics. Figure 8 shows the power dispatch of the units in the islanded mode. Comparing the curves with those in Figure 7, one can say that the microgrid has to increase the internal power generation to compensate for the power generation shortage from the upstream grid. This means higher operation cost but still, no low shedding has happened.

To optimal values of the objective functions are depicted in Figure 9. To have a fair comparison, the islanding mode operation and grid-connected mode are compared for all objectives. According to the results, the system experiences a worse situation in the islanded mode which is the price that has to pay for not letting load shedding happen in the system. Moreover, the low values of AENS and SAIDI for both modes reveal the appropriate capability of the microgrid for supporting the customers with appropriate services. The low SAIDI value shows that the customers experience low shutdown time in a year. The higher cost of the microgrid in the islanding mode shows that connection to the upstream grid is economical and can provide

**FIGURE 8** Power dispatch of units over 24 h in the islanding mode

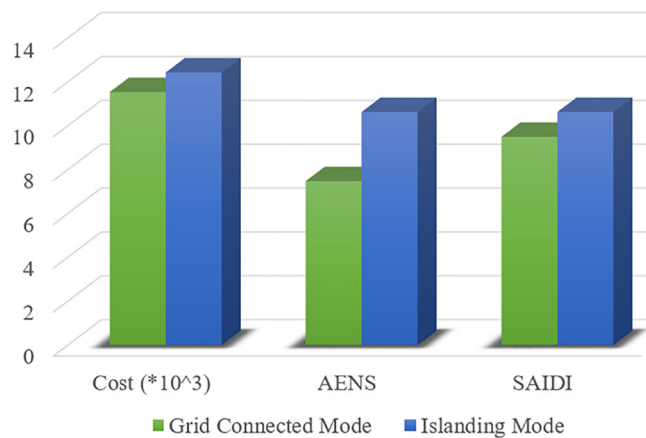
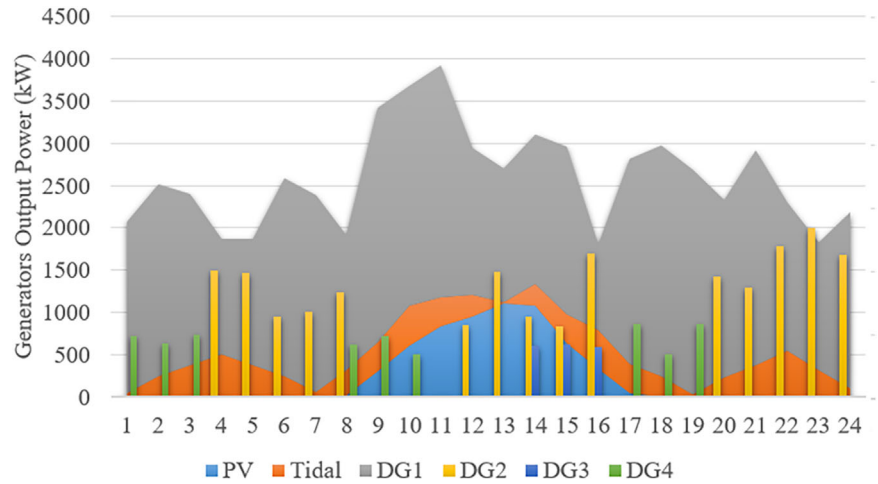


**FIGURE 9** Comparison of the cost, AENS, and SAIDI values in the islanding and grid-connected mode

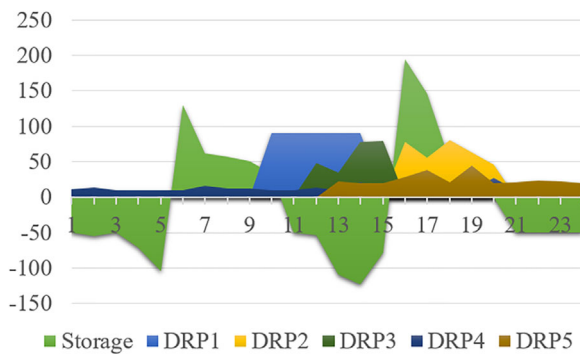


**FIGURE 10** Demand response program and the storage system status

more benefits for the microgrid owner by providing cheaper electricity. Finally, the status of the candidate loads for DRP as well as the battery charging/discharging mode are plotted in Figure 10. It is seen from the figure that the electrical loads are distributed at different hours depending on the flexibility and the total energy needed over a day. Moreover, the storage unit has actively attended the power dispatch plans to mitigate the total cost and enhance the reliability indices.

## 5 | CONCLUSIONS

This article develops a predictive-based optimal scheduling framework for the renewable microgrids considering the DRP. Different renewable energy resources of photovoltaic and tidal units are modelled and predicted in the system. A novel intelligent optimization method based on CFA and GAN is proposed to solve the problem optimally. The simulation results on the IEEE test system show that the proposed GAN model overcomes the AR, ANN, and SVR for prediction of the PV and tidal unit output power by providing lower MAPE and RMSE values. From the optimization point of view, the proposed optimizer could schedule the units in both islanding and grid-connected modes. Moreover, it is able to schedule the battery storage over 24 h in collaboration with the DRP. Five different loads which attended the DRP showed mitigating effects on the total cost by distributing their total electrical energy demand over some hours. From the reliability point of view, the proposed framework could enhance the system reliability by reducing the AENS and SAIDI. Despite all of the novel methods and simulations in this paper, several other assumptions and methods can be considered as future work. For instance, in future works electric vehicles and energy storage devices can be considered or the results of the GAN can be compared with other deep learning methods like long short-term memory and convolutional neural networks. Additionally, other reliability indices like system average frequency interruption index are considered for future work.

## FUNDING

None

## CONFLICT OF INTEREST

There is no Conflict of Interest

## DATA AVAILABILITY STATEMENT

Data available on request from the authors

## NOMENCLATURE

min/max Least/max values

B/ m,n	Set of buses in the microgrid
ch/dch	charge and discharge status
D/ d	Set of DRP loads
G/ i	Set of DGs
l	Index for CFA iteration
L/mn	Set of feeders
Q/ q	Set of feeders in a loop
S/ s	Set of batteries

## SETS

T/t Set of hours

## PARAMETERS/VARIABLES

$I_s$	source intensity
$\Gamma$	Annual outage time of component
$\zeta$	Adjustable load state
$\omega_L$	Number of loops in the microgrid
$\Delta$	Attractiveness of firefly
$\varphi_1$	Random value in the range [0,1].
$\Phi^M$	Cost of energy purchased from the main grid
$\gamma$	Absorbion coefficient
$\chi^1, \chi^2$	Switching indicators
$\mathfrak{R}^u / \mathfrak{R}^D$	Ramp down/up rate
B	Battery energy
DT/UT	Minimum down/up time
E	Adjustable load total required energy
F(.)	DG production cost
I	Commitment state of dispatchable units
$I_0$	original light intensity
Lc	Average bus load
MC/MD/MU	Minimum charging/discharging/operating time
$M_D$	Mean of the population
$N^C$	Number of customers
NL	Number of lines to form a loop
$N^{\max}_{\text{switching}}$	Maximum switching actions for each switches.
P	DG output power
PD/QD	Active/Reactive load demand
PL/QL	Active/Reactive line power flow
$P^M$	Main grid power
R	Distance between two fireflies
Rand	uniformly distributed generated number in [0,1].
T	Scheduling horizon
T <sup>ch/dch</sup>	Number of successive charging/discharging hours
T <sup>on/off</sup>	Number of successive ON/OFF hours
u/v	Energy storage discharging/charging state
$u^M$	Islanding state of the microgrid
V/ $\delta$	Bus voltage magnitude/phase
W	Weighting factor of the sample point
$X_g$	Best solution in CFA
Y/ $\theta$	Magnitude/phase of line admittance
$\alpha$	randomization parameter
$\beta$	Open/closed state of the switch
$\epsilon / \nu$	Start time/end time of adjustable loads
$\eta$	Energy storage efficiency

$\lambda^{\text{RCS}}$  Hourly switching operation cost

$\tau$  Time period

## ORCID

Mobammadamin Mobtabej  <https://orcid.org/0000-0001-8963-6723>

## REFERENCES

- Mohammadi, M., Kavousi-Fard, A., Dabbaghjamesh, M., Farughian, A., Khosravi, A.: Effective management of energy internet in renewable hybrid microgrids: A secured data driven resilient architecture. IEEE Trans. Ind. Inf. (in press). <https://doi.org/10.1109/TII.2021.3081683>
- Aflaki, A., Gitzzadeh, M., Razavi-Far, R., Palade, V., Ghasemi, A.A.: A hybrid framework for detecting and eliminating cyber-attacks in power grids. Energies 14(18), 5823 (2021)
- Lei, M., Mohammadi, M.: Hybrid machine learning based energy policy and management in the renewable-based microgrids considering hybrid electric vehicle charging demand. Int. J. Electr. Power Energy Syst. 128, 106702 (2021)
- Shirsat, A., Tang, W.: Quantifying residential demand response potential using a mixture density recurrent neural network. Int. J. Electr. Power Energy Syst. 130(1), 13–54 (2021)
- Gabaldón, A., García-Garre, A., Fernandez-Jimenez, L.A.: Improvement of customer baselines for the evaluation of demand response through the use of physically-based load models. Utilities Policy 101213, 70, (2021)
- Hamw, M., Lizarralde, I., Legardeur, J.: Demand response business model canvas: A tool for flexibility creation in the electricity markets. J. Cleaner Prod. 282, 124539 (2020)
- Ur Rehman, A., Lie, T.T., Tito, S.R.: Non-invasive load-shed authentication model for demand response applications assisted by event-based non-intrusive load monitoring. Energy AI 3(1), 14–22 (2021)
- Mohseni, S., Brent, A.C., Burmester, D.: Strategic design optimisation of multi-energy-storage-technology micro-grids considering a two-stage game-theoretic market for demand response aggregation. Appl. Energy 287, 116563 (2021)
- Kaluthantrige, R., Rajapakse, A.D.: Demand response integrated day-ahead energy management strategy for remote off-grid hybrid renewable energy systems. Int. J. Electr. Power Energy Syst. 129, 106731 (2021)
- Liu, Z., Zhao, Y., Wang, X.: Long-term economic planning of combined cooling heating and power systems considering energy storage and demand response. Appl. Energy 279, 1–18 (2020)
- Elkasrawy, A., Venkatesh, B.: Positive demand response and multi-hour net benefit test. Electr. Power Syst. Res. 183, 106275 (2020)
- Nayak, A., Maulik, A., Das, D.: An integrated optimal operating strategy for a grid-connected AC microgrid under load and renewable generation uncertainty considering demand response. Sustainable Energy Technol. Assess. 45, 101169 (2021)
- Kavousi-Fard, A., Khodaei, A.: Efficient integration of plug-in electric vehicles via reconfigurable microgrids. Energy 111, 653–663 (2017)
- Curto, D., Martín, M.: Renewable based biogas upgrading. J. Cleaner Prod. 224, 50–59 (2019)
- Cheng, T., Zhu, X., Gu, X., Yang, F., Mohammadi, M.: Stochastic energy management and scheduling of microgrids in correlated environment: A deep learning-oriented approach. Sustainable Cities Soc. 69, 102856 (2021)
- Kavousi-Fard, A., Mohammadi, M., Al-Sumaiti, A.S.: Effective strategies of flexibility in modern distribution systems: reconfiguration, renewable sources and plug-in electric vehicles. Flexibility in Electric Power Distribution Networks, pp. 95–119. CRC Press, Boca Raton, FL (2021)
- Kavousi-Fard, A., Niknam, T., Akbari-Zadeh, M.R., Dehghan, B.: Stochastic framework for reliability enhancement using optimal feeder reconfiguration. J. Syst. Eng. Electron. 25(5), 901–910 (2016)
- Kavousi-Fard, A., Niknam, T., Baziar, A.: A novel multi-objective self-adaptive modified  $\theta$ -firefly algorithm for optimal operation management of stochastic DFR strategy. Int. Trans. Electr. Energy Syst. 25(6), 976–993 (2015)

19. Kabir, H.M.D., Khosravi, A., Nahavandi, S., Kavousi-Fard, A.: Partial adversarial training for neural network-based uncertainty quantification. *IEEE Trans. Emerg. Top. Comput. Intell.* 5(4), 595–606 (2021)
20. Dabbagh, M., Kavousi-Fard, A., Zhen, Y.: Stochastic modeling and integration of plug-in hybrid electric vehicles to microgrids. *IEEE Trans. Intell. Transp. Syst.* 22(7), 4394–4403 (2021)
21. Tajalli, Z., Mardaneh, M., Taherian-Fard, E., Izadian, A., Kavousi-Fard, A., et al.: DoS-Resilient Distributed Optimal Scheduling in a Fog Supporting IIoT-based Smart Microgrid. *IEEE Trans. Ind. Appl.* 56(3), 2968–2977 (2020)

**How to cite this article:** Mobtahej, M., Esapour, K., Tajalli, S.Z., Mohammadi, M.: Effective demand response and GANs for optimal constraint unit commitment in solar-tidal based microgrids. *IET Renew. Power Gener.* 16, 3485–3495 (2022).  
<https://doi.org/10.1049/rpg2.12331>